5-2022

Regulation of the Reaction Between Cytochrome c and Cytochrome c Oxidase in the Mitochondria

Anders Nowell

Regulation of the Reaction Between Cytochrome c and Cytochrome c Oxidase in the Mitochondria

An Honors Thesis submitted in partial fulfillment of the requirements for Honors studies in Biology

By

Anders Nowell

Spring 2022

Biology

J. William Fulbright College of Arts and Sciences

The University of Arkansas

Acknowledgements

The research in this thesis was sponsored by the Department of Chemistry and Biochemistry at The University of Arkansas, Fayetteville, under the supervision of Dr. Frank Millett. The project was funded by NIH grants GM20488 and 8P30GM103450, and the Bruker Professorship. This project would not have been possible without Marti Scharlau and Dr. Frank Millett and their help with research and understanding results.

Table of Contents

Abstract

Cytochrome c (Cc) is a multifunction protein that has important life and death functions in the cell. In the electron transport chain (ETC), Cc transfers electrons from cytochrome bc_1 to cytochrome c oxidase (CcO), which helps build the electrochemical gradient that drives ATP synthase. The reaction of Cc with CcO is very important in ETC regulatory processes. Previous research shows phosphorylation sites in Cc that affect the binding with CcO, with measurable effects on k_d, k_f, and K_D. These effects result in changes in mitochondrial membrane potentials, respiration, and reactive oxygen species (ROS) scavenging. This research involved a new phosphorylation site on Cc, Tyr 46. Using site-directed mutagenesis, we mutated tyrosine to a glutamate residue. Steady-state kinetic and analytical ultracentrifuge experiments were performed to examine the binding strength of the Cc:CcO complex. Results showed slight differences between Y46E and WT Human Cc, possibly indicating that Y46E changes the binding complex. However, the differences were small enough to say that Y46E had no significant effects on the Cc:CcO binding complex.

Introduction and Purpose

The Electron Transport Chain

Cytochrome c (Cc) is a 12kDa, 104 amino acid globular protein with an attached heme group that participates in cell respiration processes such as electron shuttling in the mitochondrial electron transport chain, as well as other functions like ROS scavenging and apoptosis. The electron transport chain is a key player in cellular metabolism, specifically in aerobic respiration to catabolize glucose into adenosine triphosphate (ATP). The electron transport chain is made up of five protein complexes that are integrated within the inner mitochondrial membrane. Complex I (NADH-ubiquinone oxidoreductase) transfers electrons from the mitochondrial matrix to ubiquinone via NADH. These electrons are passed to ubiquinone (Q) where they eventually enter the Q cycle resulting in the reduction of Q to ubiquinol (QH_2). 4 Protons (H^+) are then pumped into the mitochondrial intermembrane space to begin building a concentration gradient. Complex II (succinate dehydrogenase) first catalyzes the oxidation of succinate to fumarate in the TCA cycle and donates electrons from succinate to CoQ via $FADH_2$. Unlike Complex I, complex II does not pump H^+ into the intermembrane space. Complex III (cytochrome bc_1 complex/ cytochrome c reductase) transfers electrons from QH_2 to Cc. After completion of the Q cycle, four more H^+ ions are pumped into the intermembrane space. Complex IV (cytochrome c oxidase) transfers electrons from Cc to the final electron acceptor, O_2, which generates H_2O. In complex IV, 2 H^+ ions are pumped where they are used to form one H_2O from ½ O_2, and $2H^+$ are pumped into the intermembrane space. Complexes I, II, and III together carry out the electron transfer reaction $NADH + ½\ O_2 + H^+ \rightarrow\ NAD^+ + H_2O$ and use that energy to pump 10 protons from the mitochondrial matrix to the intermembrane space to form a membrane potential of $V_{in} - V_{out} \approx -0.14$ V and a pH gradient of $pH_{in} - pH_{out} \approx +1.4$.

Complex V is the ATP synthase which uses the energy of the membrane potential ΔV and pH gradient ΔpH to drive ATP synthase rotation, which adds a phosphate to ADP to synthesize ATP (Zhao, Jiang, Zhang, & Yu, 2019). The overall steps of the ETC and oxidative phosphorylation are shown in **Figure 1.**

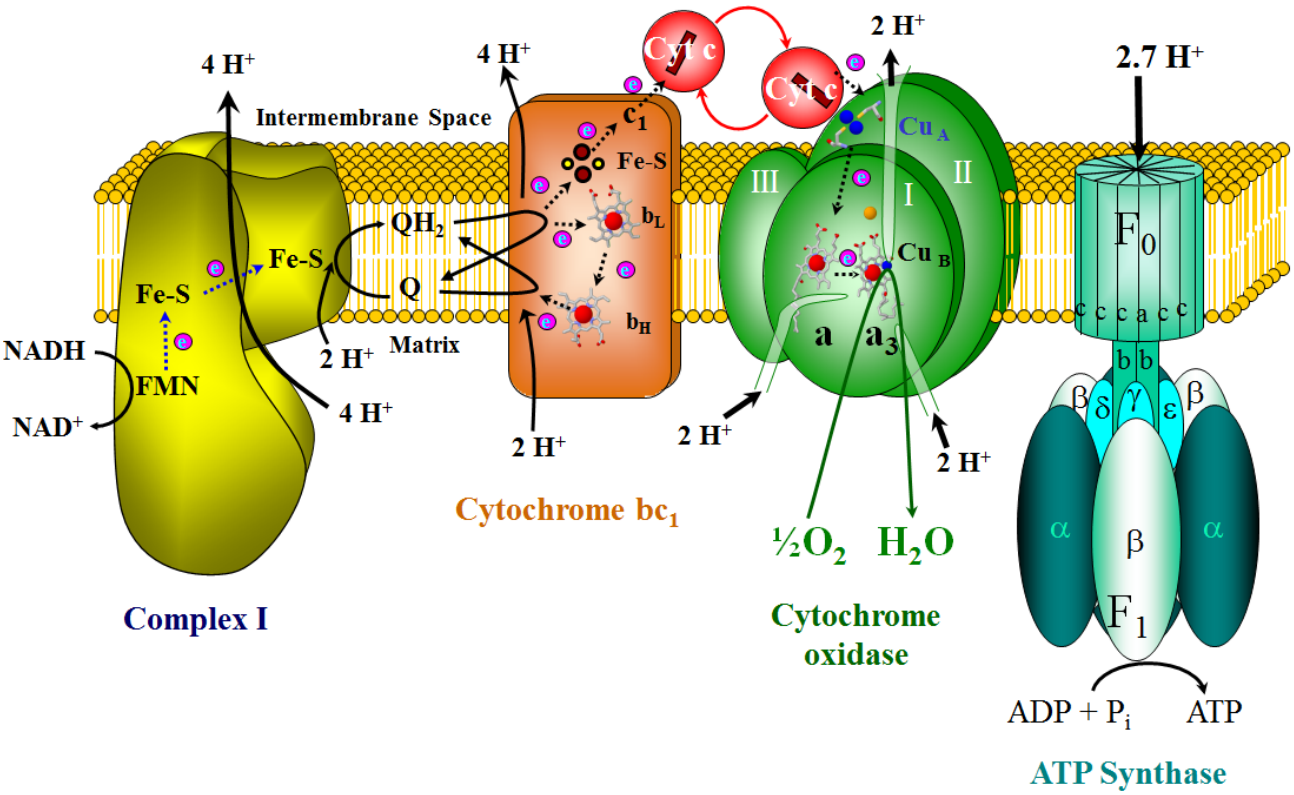

Figure 1. Overview of mitochondrial oxidative phosphorylation (Millett slide)

The complexes of the ETC have been subject to years of detailed study, and each complex has an important role in aerobic respiration.

Cytochrome c

The main area of this research involves cytochrome c, which transfers electrons from cytochrome bc_1 to cytochrome oxidase in the ETC. Cc is also a multifunctional enzyme that is involved in both life and death decisions in a cell. These functions are summarized in **Figure 2** and include apoptosome formation in apoptosis, cardiolipin peroxidase, supercomplex assembly, ROS scavenging, and most significantly for this research, ETC regulation through cytochrome c oxidase (CcO) interactions.

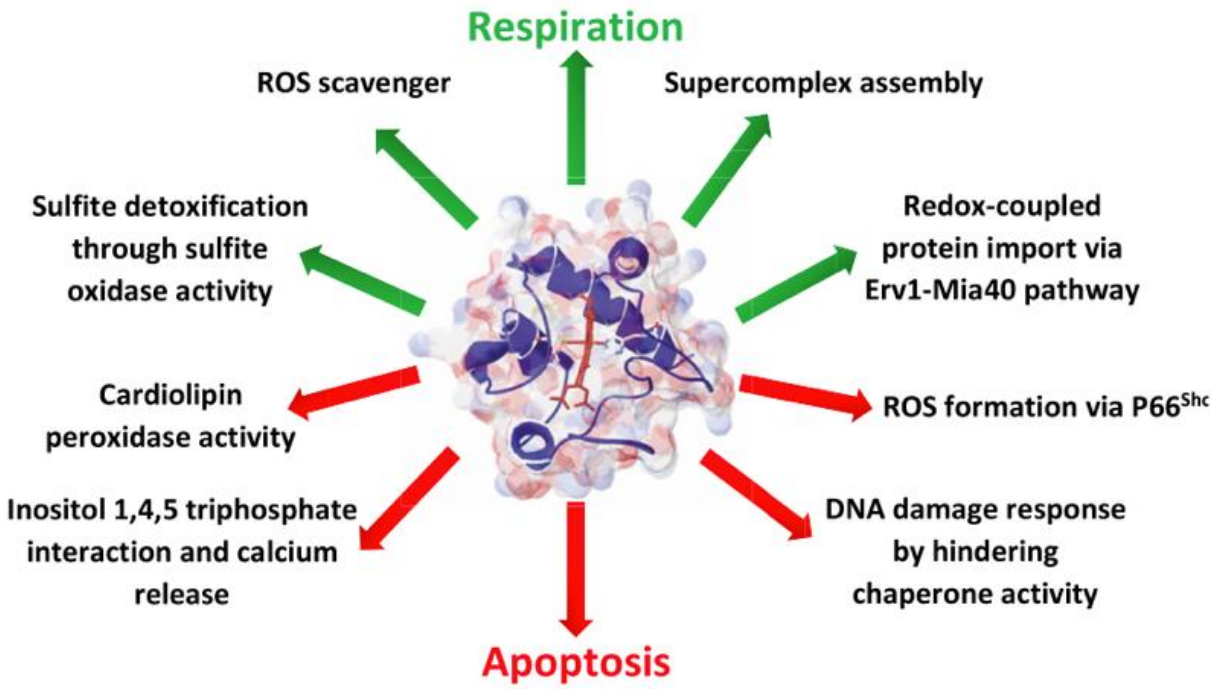

Figure 2. Life and death functions of Cc highlighted in green and red respectively (Kalpage, et al., 2019)

Certain residues in Cc are phosphorylated in highly specific manners, which adjust mitochondrial membrane potential to minimize ROS production. In stressful conditions such as ischemia-reperfusion injuries, these phosphorylations are lost resulting in membrane potential hyperpolarization and excessive ROS generation (Hüttemann, et al., 2011)**.** (Hüttemann, et al., 2012)

Cytochrome c and cytochrome c oxidase interactions

The heme group of Cc is wrapped in a hydrophobic crevice which allows it to efficiently exchange electrons with redox partners (Hüttemann, et al., 2011) . In oxidative phosphorylation, the interaction between Cc and CcO is very important. The interaction must rapidly form a highly specific complex and stabilize the optimal orientation of the two complexes for rapid electron transfer. Previous studies indicate a highly electrostatic interaction between the two proteins and experimental modifications have shown that seven lysine amino groups surrounding the heme crevice of Cc are involved in the interaction with COX (Scharlau, et al., 2019) The most accepted model of the Cc:CcO complex was proposed by Roberts and Pique in 1999. This computational docking model is shown in **Figure 3.** Interactions of Cc Lys13 with CcO Asp119 and Cc Lys72 with CcO Gln103 and Asp158 are very critical due to their proximity to the hydrophobic region. In this model, the proposed electron transfer pathway is:

heme c $\rightarrow$ CcO Trp-104 $\rightarrow$ Cu_A $\rightarrow$ heme a $\rightarrow$ heme a_3 which is supported by kinetics studies (Smith, Ahmed, & Millett, 1981).

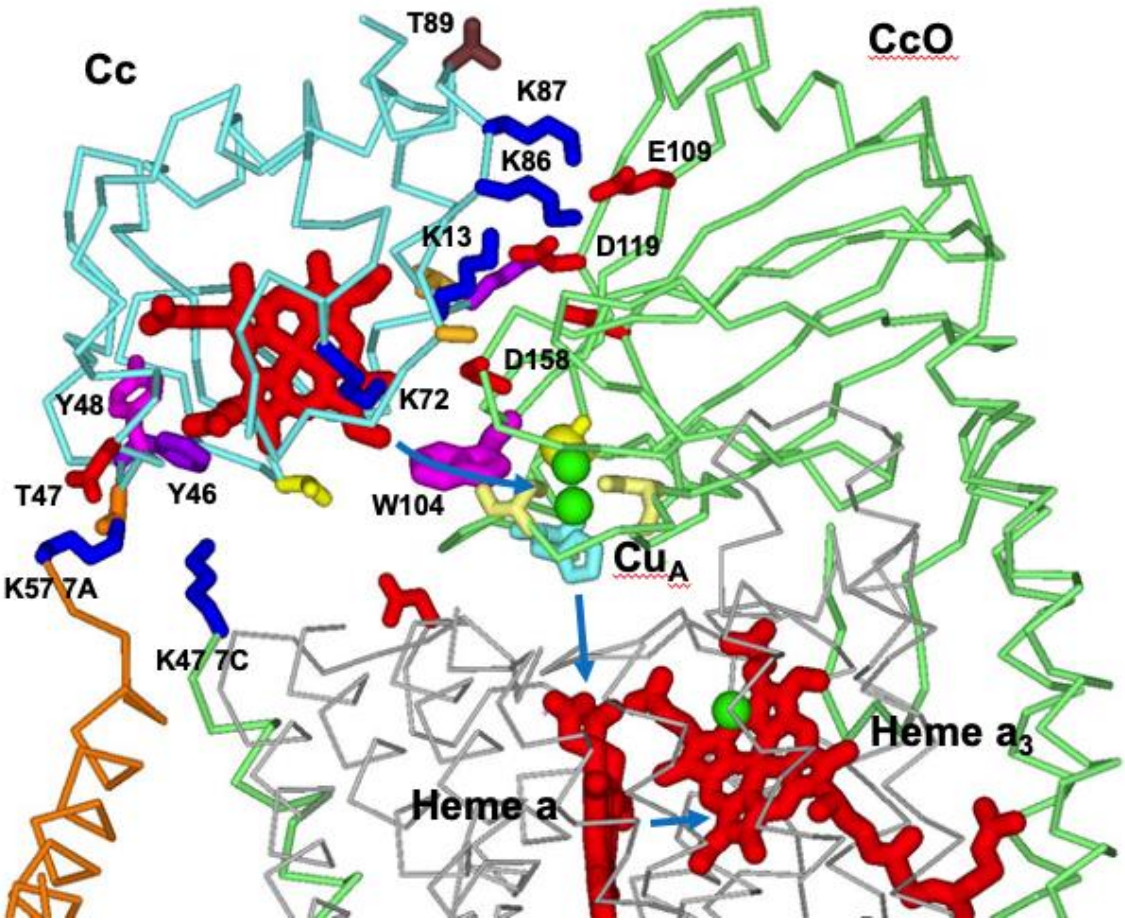

Figure 3. Computational model of Horse Cc:Bovine CcO binding complex determined by crystal structures of each protein. Positively charged lysine residues are colored in blue, and negatively charged glutamate and aspartate residues are colored in red. The proposed electron transfer pathway is indicated by the blue arrows (Roberts & Pique, 1999).

Recently, a new X-ray crystal structure of the Cc:CcO complex has been proposed that drastically differs from the computational model (Shimada, et al., 2017). This can be seen in **Figure 4**.

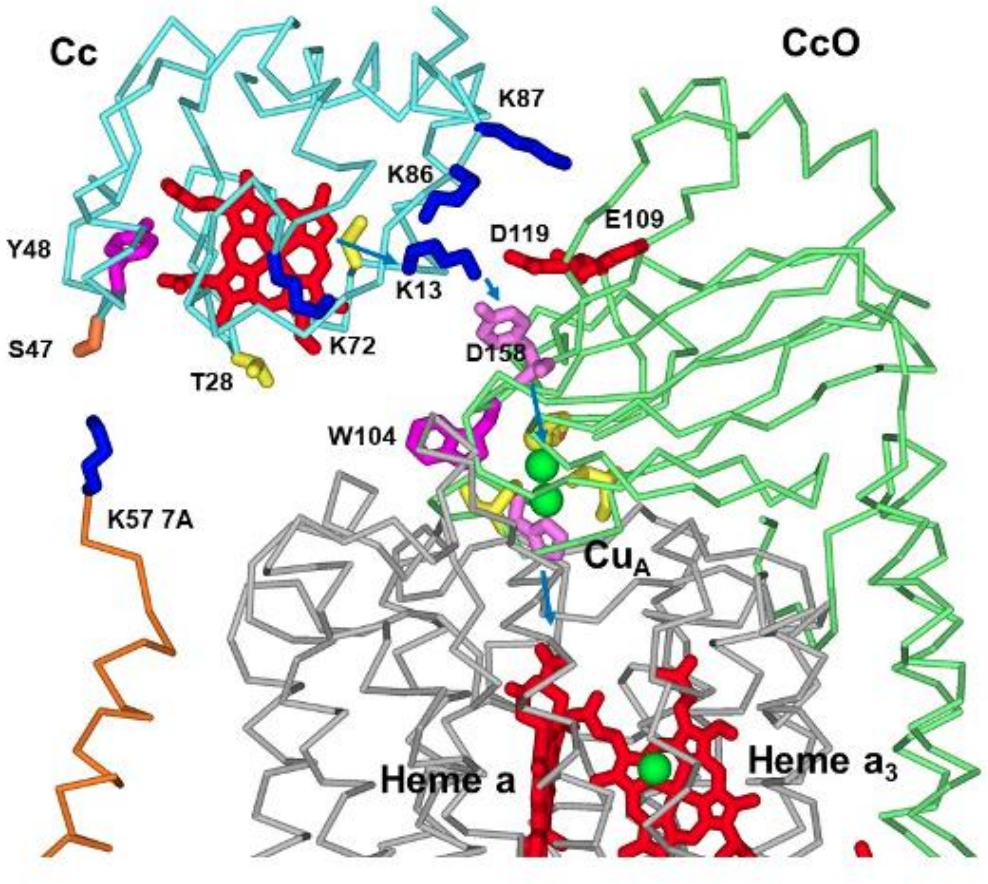

Figure 4. X-ray crystal structure of horse Cc:Bovine CcO (Shimada, et al., 2017)

In this structure, Cc is far away from CcO, typically uncharacteristic of protein-protein binding. This structure also does not line up with extensive steady-state and mutagenesis studies regarding the Cc:CcO complex, and so it is assumed that the most accepted model still comes from **Figure 3.**

Phosphorylation sites on cytochrome c

Currently, five phosphorylation sites of Cc have been characterized: Tyr97, Tyr48, Thr28, Ser47, and Thr58. All five have been shown to inhibit respiration, which results in a stabilized

mitochondrial membrane along with low ROS production. During periods of ischemic stress, these phosphorylations are lost resulting in mitochondrial membrane flux, ROS generation, and apoptosis (Kalpage, et al., 2020).

Tyrosine-97

First, Tyr 97 was found to be phosphorylated in bovine heart tissue. This phosphorylation shifted the 695 nm heme-iron-Met^{80} band to 687nm, indicating that the heme environment of Cc was changed. (Lee, Salomon, Doan, Grossman, & Hütteman, 2006). Another study mutated Tyr 97 to Y97E which resulted in decreases in protein stability determined by melting temperature analysis. This was most likely a result of the loss of the aromatic ring present in tyrosine (García-Heredia, et al., 2011). Another study more relevant to the current research mutated Tyr 97 with a p-carboxymethyl-phenylalanine (pCMF) which resulted in increased CcO activity compared to wild-type *in vivo* Tyr 97 (Guerra-Castellano, et al., 2018).

Tyrosine-48

Tyr 48 was then mapped to be phosphorylated in bovine liver (Yu, Salomon, Yu, & Hüttemann, 2008). Using the phosphomimetic mutant Y48E, it was found that turnover rates in the reaction with liver CcO were reduced by 50%, while midpoint redox potential was also decreased. (Pecina, et al., 2010) Other studies add onto this evidence and indicate Tyr48 most likely has an important role in electron transfer and ROS scavenging.

Threonine-28

Phosphorylated Thr 28 was then mapped in bovine kidney, where 80% of purified bovine Cc were found to have phosphorylated Thr 28. A 50% decrease in CcO activity was observed in vivo, while a 73% decrease in CcO activity was observed in the phosphomimetic T28E mutant. (Mahapatra, et al., 2017) Interestingly, cells with the T28E Cc mutant showed lower mitochondrial membrane potentials and ROS levels indicating that this mutation partially inhibits mitochondrial respiration (Kaim & Dimroth, 1999) (Kalpage, et al., 2019).

Threonine-58

Phosphorylated Thr 58 in rat kidney (which is replaced with isoleucine in humans) has been shown to lower CcO activity, lower redox potential, have a lower rate of oxidation, and have a lower membrane potential. The phosphomimetic mutant T58E was shown to be more resistant to heme degradation and serve as a better ROS scavenger than T58. (Wan, et al., 2019).

Serine-47

Finally, Ser 47 has been found to be phosphorylated in rat and porcine brain under basal conditions This phosphorylation lowers apoptotic activity under health conditions, while preventing high respiration rates leading to mitochondrial membrane potential hyperpolarization. (Kalpage, et al., 2019) (Sanderson, Reynolds, Kumar, Przyklenk, & Hüttemann, 2013b).

These Cc phosphorylation sites and their structural interactions with COX can be seen in **Figure 5.**

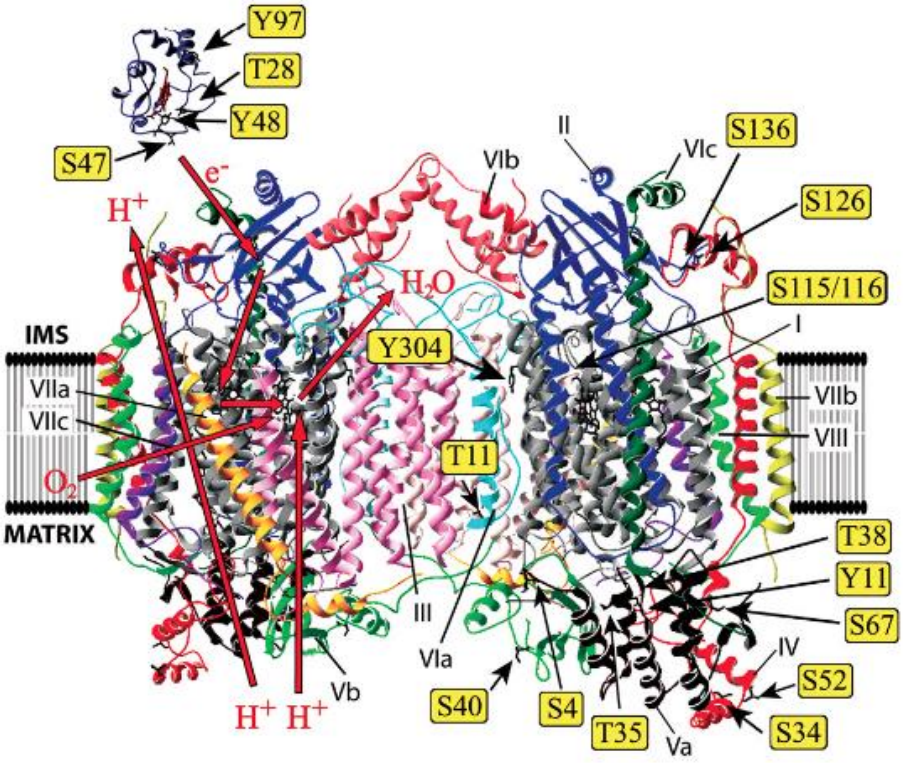

Figure 5 . Mapped phosphorylation sites on cytochrome c and cytochrome c oxidase (Hüttemann, et al., 2012)

Current Research

Further study of Cc phosphorylations could give key insight into how Cc and CcO interact and the physiological effects that they have on each other. This research will focus on another residue of Cc, Tyrosine-46. Using site directed mutagenesis methods, we mutated the tyrosine residue to a glutamate residue. Using a phosphomimetic mutant we were able to study the binding kinetics of Cc with CcO using steady state and analytical ultracentrifuge methods. Due to its proximity to

CcO, Y46 on Cc could potentially have effects on Cc:CcO binding if mutated. It is located relatively close to Threonine 47 on Cc as shown in **Figure 3**, and so this research aims to study those potential binding effects. Tyrosine is an aromatic amino acid with a hydroxyl group, while glutamate is a linear amino acid with an attached negatively charged carboxylate group. The mutation of tyrosine to glutamate is called a phosphomimetic mutation since the negatively charged glutamate mimics a phosphorylated tyrosine. Structural and charge differences in these amino acids could influence binding kinetics. Upon purification of a mutated protein, the mutant will be compared to wild-type Cc to determine if the electron transfer kinetics have changed. As determined by previous papers, phosphorylations at Y48 and S47 have shown effects on membrane potentials, ROS scavenging, and respiration rates. Study of the Y46E mutation could potentially reveal valuable information regarding effective control mechanisms for mitochondrial diseases.

Materials and Methods

Site directed mutagenesis

To design our specific Cc mutant, we utilized the QuikChange II mutagenesis kits from Agilent technologies. Using their primer design tool, we input our protein sequence for both the wild type and mutant Cc and then ordered the primer from Integrated DNA Technologies. In position 46 of Cc, we replaced the "TAC" codon to "GAA" to change the amino acid at that position from tyrosine (Y) to glutamate (E). These designed sequences are shown in **Table 1.**

Wild Type	5'- C CAG GCG CCG GGC ***TAC*** AGC TAC ACG GCGG - 3'
Y46E Sense	5'- C CAG GCG CCG GGC ***GAA*** AGC TAC ACG GCG G -3'
Y46E Anti-Sense	3'- G GTC CGC GGC CCG ***CTT*** TCG ATG TGC CGC C -5'

Table 1. Amino acid sequences for Wild Type, Y46E sense and Y46E anti-sense Cc

Once the primers arrived, procedures for insertion into the human cytochrome c plasmid were followed. First, they were pulse centrifuged and then 0.8 ml of sterile water was added to each. They were incubated for two hours then stored at -20°C. After thawing, the primer concentration was determined by adding 5 µl of each primer to a cuvette with 495 µl water. Using a spectrophotometer [1], the absorbances were read at 260 nm. The absorbance @260 nm=1 for 33 µg/ml single stranded DNA, so A@260nm x33= DNA in µg/ml in each cuvette. This value was multiplied by 100 to calculate DNA in stock solution for each primer. Plasmids were then diluted to 1:100 (5 µl plasmid in 495 µl sterile distilled water) and absorbances were read at 260 nm. Several tubes per mutated plasmid were set up, and plasmid concentrations were varied with a

[1] Hewlett Packard 8452A Diode Array Spectrophotometer paired with the software from Agilent Technologies. UV-Visible ChemStation Rev. A.10.01 copyright Agilent Technologies 95-03

final total reaction volume [2] always at 50 µl. Using the thermocycler, PCR reactions were run for 4 hours. After thermal cycling, µ1 L of Dpn1 restriction enzyme was added to digest the parent DNA. The mutated plasmid was then incubated at 37°C for one hour.

Transformation and plasmid preparation

5µl Dpn-1 treated DNA was added to a pre-chilled Falcon 2054 polypropylene tube. *E. Coli* XL-1 Blue super competent cells were thawed on ice, and then 50 µl of the treated DNA was mixed in and incubated on ice for 30 minutes. After incubation, the mix was heat pulsed at 42° C for 45 seconds, then put back on ice for 2 minutes. 0.5 ml NZY+ [3] broth was added and then incubated at 37°C for 1 hour with 225-250 rpm shaking. The cell suspension was then placed on a LB agar plate containing ampicillin and incubated at 37°C overnight. After incubation, the approximate number of colonies were noted. 5 µl of ampicillin was then added to each of fourteen tubes containing broth. Single colonies were removed from the plates and placed into each culture tube. The tubes were incubated overnight in a shaker at 37°C and then prepped using the Wizard Plus Miniprep DNA Purification System. After preparation, plasmids were sent to a DNA sequencing lab [4] to determine if mutation attempt was successful. The plasmid was then stored at -80°C until next steps.

[2] __Sterile Water + 6 µL primer1 + 6 µL primer2 + 5µl 10x Pfu reaction buffer + 1µl dNTP + __µL plasmid + 1µL Pfu DNA polymerase (2.5 U/ml)
[3] NZY+ Broth- 12.5 µL M $MgCl_2$ + 12.5 µL 1 M $MgSO_4$ + 20µL 20% Glucose
[4] UAMS

Expression of Mutated Cytochrome c and Purification

Terrific Broth [5] was used for large scale growth and expression of mutants. 2 μl of choice plasmid was added to a pre-chilled falcon tube along with 25 μl E. Coli stock (BL21DE3). After incubation on ice, the solution was heat pulsed. Broth was then added for incubation. The cells were then spread on an ampicillin agar plate and incubated for 24 hours. After 24 hours, colonies were picked from the plate and dropped into a 6L flask containing 2L of sterile terrific broth containing 2 ml of ampicillin. Three colonies were picked per flask. After placing on orbital shakers, the flasks were incubated for 48 hours. Cells were harvested by centrifuging at 10,000 rpm for 15 minutes. After weighing, the cells were then resuspended in lysis buffer [6]**.** 3 ml of lysis buffer and 9 mg lysozyme were added per gram of cell paste. A small amount of DNase was added and then the mix was stirred for one hour. Cells were then frozen at -80°C overnight. After thawing, cells were centrifuged at 18,000 rpm. The supernatant containing protein was kept, and ammonium sulfate was added to a concentration of 50% saturation. The mix was centrifuged at 10,000 rpm and the supernatant was kept. Ammonium sulfate was added to a concentration of 90% saturation and centrifuged again. After centrifugation, the pellet was kept and then placed in a dialysis bag with 12000-14000 MWCO against 2L of 10-50 mM Tris buffer. This allows the protein to refold. Dialysate was then loaded onto cold room columns [7]. Tubes with 410 abs higher than 280 abs were kept. After exchanging with buffer, tubes were exchanged with 5mM P_i before running on HPLC for final purification.

[5] Per One Liter: 11.8g Tryptone, 23.6g Yeast extract, 9.4g Dipotassium hydrogen phosphate, 2.2g Potassium dihydrogen phosphate, 4mL Glycerol (0.4%)
[6] Lysis Buffer: 50ml 1M Tris pH 8, 50ml 100mM EDTA, 10ml 1M $MgSO_4$, 1ml 1M $CaCl_2$ (Brought to 1L with distilled water)
[7] S-Sepharose cation-exchange column; pre-equilibrated with 50mM Tris

HPLC

High performance liquid chromatography was used in the final step for final purification of Cc. The Cc sample was oxidized with potassium ferricyanide [8] and then loaded onto a BioRad UNOS12R cation exchange column. The HPLC gradient can be seen in **Table 2.**

Time (minutes)	% 5mM P_i pH 6	% 500mM P_i pH 6
0	100	0
5	80	20
60	0	100
65	0	100
80	100	0

Table 2: HPLC gradient used for BioRadUNOS12R Column

Chromatograms produced from HPLC shown a large 410 nm peak around 42 minutes, which is where most of our purified sample was taken from. This is seen in **Figure 6.**

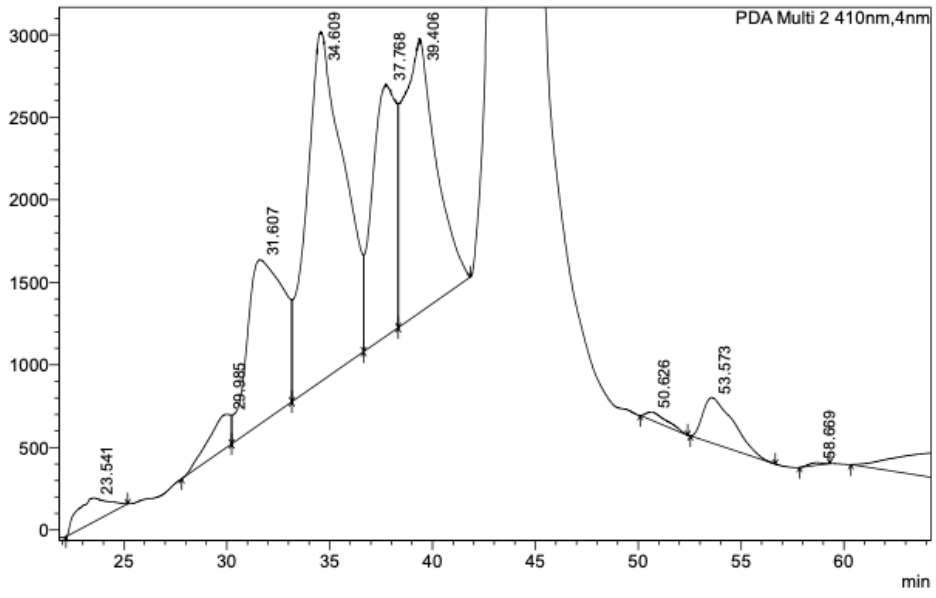

Figure 6. BioRad UNOS12R Chromatogram

[8] $(K_3Fe(CN)_6)$

A second gradient was then used on a smaller BioRadUNOS1 column to verify purity of the Cc sample. Gradient conditions for this run can be seen in **Table 3.**

Time	% 5mM P_i pH 6	% 500mM P_i pH 6
0	100	0
3	80	20
30	0	100
32	0	100
40	100	0

Table 3. HPLC gradient used for BioRadUNOS1 Column

A produced chromatogram from this gradient shows a 410 nm peak at around the 20-minute mark, indicating a pure Cc sample. This is seen in **Figure 7.**

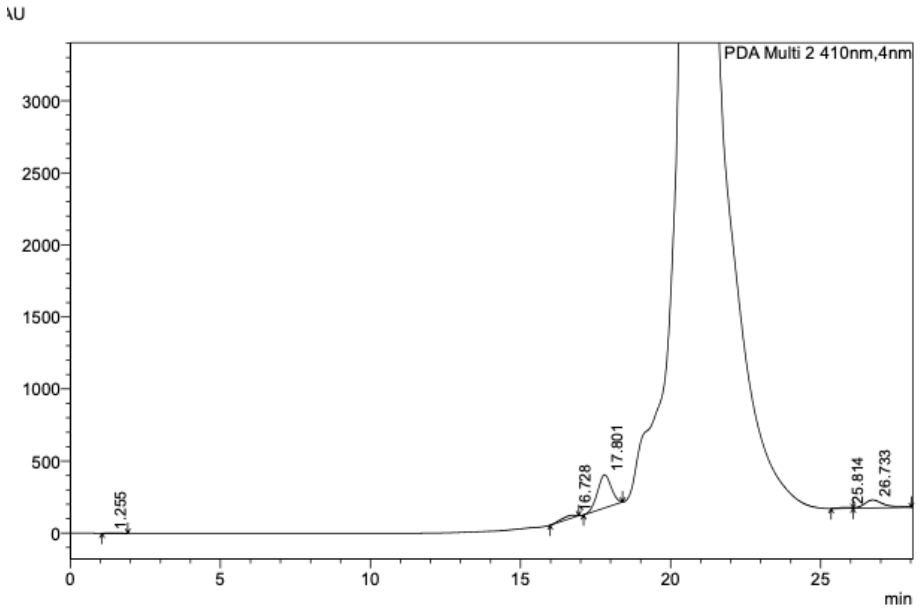

Figure 7. BioRadUNOS1 Chromatogram

Readings were obtained at 280 nm, 410 nm, and 542 nm and fractions were collected by an automated fraction collector [9]. Tubes containing concentrated Cc were stored at -80°C until use in experiments.

[9] Shimadzu SPD-M20A Diode Array Detector

Steady State Kinetics

Before each run, quartz cuvettes were filled with 300 µl of buffer (either low ionic strength [10] or high ionic strength [11] depending on experiment), and the spectrophotometer was blanked to create a baseline measurement. For each run, varying volumes of Cc were added to the buffer to reach a Cc concentration of around 0.50 µM. The amount of Cc added varied on the concentration levels of the various test species: WT Human Cc, WT Horse Cc, or Y46E Cc. The kinetics software measured the absorbance at 550 nm and 542 nm, and then **Equation 1** was used to determine the concentration of Cc in the cuvette.

$$\frac{Au\ 550nm - Au\ 542}{17.8} \times\ 1000$$

Equation 1. Cc Concentration with extinction coefficient= 17.8

Catalytic volumes of CcO were then added and quickly shaken into the cuvette. Measurements were taken immediately after the CcO was added, and then one spectrum was taken per second for 360 seconds. All Cc:CcO concentrations were based on Beer's law [12], but simplify to **Equation 2** due to our path length being 1cm.

$$C = \frac{A}{\varepsilon}$$

Equation 2. Simplified Beer's law where C is concentration, A is absorbance, and ε is the extinction coefficient.

[10] 2mM P_i pH 7
[11] 20mM P_i with 200mM NaCl
[12] Beer's Law: $A = \varepsilon bC$

The Bovine CcO concentration was calculated from pre-determined aliquots of CcO that have been prepared for steady-state experiments. Each day, a fresh aliquot of CcO was thawed. The concentration of reduced Cc was found to decrease exponentially after the addition of CcO according to **Equation 3.**

$$CytC_{red} = CytC_{Red(initial)}e^{(-kt)}$$

Equation 3. Where k is the first order rate constant and t=time

Analytical Ultracentrifugation

The analytical ultracentrifuge experiment was used to determine the dissociation constant (K_D) between Cc and CcO. Using sedimentation coefficients, the differences between bound Cc and unbound Cc are determined. Free (unbound) Cc has a sedimentation coefficient of 1.74 S while the Cc:CcO complex has a sedimentation coefficient of 11.4 S. Experiments were performed on both the wild-type and the Y46E mutant Cc. Ultracentrifuge runs were done at multiple NaCl concentrations, starting with the sample cell containing no NaCl and moving up in concentrations to 50, 70, 130, and 350 mM of NaCl. Different NaCl concentrations change the ionic strength of the solution, which theoretically should affect the binding strength between Cc and CcO. In this experiment, there was an excess of CcO in relation to Cc to ensure that at zero salt concentration all the Cc is bound. Presumably there will also be no bound Cc to CcO at 350 μM salt concentration. 300 μl of the prepared Cc and CcO were added into the sample cell to be placed in the ultracentrifuge. The Cc and CcO concentrations were checked and confirmed using the spectrophotometer separately. Concentrations were determined by the protein's extinction coefficient at isosbestic points (points where the absorbance doesn't change when protein is reduced or oxidized), so either 420 nm or 598 nm for CcO and 410 nm or 542 nm for Cc. Each ultracentrifuge run was about an hour to an hour and 15 minutes, taking an absorbance

reading every 10 minutes. The ultracentrifuge was set to 48,000 rpm and 22 °C. After each run, salt was added to achieve the desired salt concentration. This was repeated for both the wild-type and the mutant Y46E.

Results and Discussion

Steady State Kinetics

It has been found that the reaction between Cc and CcO obeys a first order kinetic relationship at all Cc concentrations and ionic strengths (Minnaert, 1961) (Smith, Davis, & Nava, 1979). This indicates that the k_d and k_f values for $CytC^r$ and $CytC^O$ binding to CcO are equal. Therefore, the first order rate constant (k_{obs}) is equal to V/S.

With this assumption being made, Minnaert and others working on this reaction have found that the reaction between Cc and CcO occurs with the mechanism shown:

$$CytC^r + CcO \underset{k_d}{\overset{k_f}{\rightleftarrows}} CytC^r{:}CcO \xrightarrow{k_{et}} CytC^o{:}CcO^r \underset{k_f}{\overset{k_d}{\rightleftarrows}} CytC^o + CcO^r$$

To simplify this equation, let $CytC^r$ = S, $CytC^O$ = P, and CcO = E E_t = total E

$$S + E \underset{k_d}{\overset{k_f}{\rightleftarrows}} S{:}E \xrightarrow{k_{et}} P{:}E \underset{k_f}{\overset{k_d}{\rightleftarrows}} P + E$$

Under steady-state kinetic conditions, the rate constant V = dS/dt for this reaction is:

$$V = k_f k_d k_{et} [S]E_t/\{k_f(k_d + k_{et})[S + P] + k_d(k_d + k_{et})\}$$

Previous studies in the lab of Francis Millett have established that $k_{et} >> k_d$. Therefore, the simplified equation is valid:

$V = k_d SE_t/((S + P) + k_d/k_f)$.Since the reaction between Cc and CcO has been established to obey first order rate kinetics at all concentrations and ionic strengths, the first order rate constant is $k_{obs} = V/S$. Given this the equation becomes:

$$k_{obs} = k_d E_t/((P + S) + k_d/k_f)$$

The ratio of k_d to k_f is equal to the equilibrium dissociation constant K_D of the Cc:CcO complex. The equilibrium constant is found as:

$$k_d/k_f = K_D = [Cc][CcO]/[Cc:CcO].$$

Since at low ionic strength the association between Cc and CcO in the Cc:CcO complex is very tight, and the K_D is very small the equation can then be simplified as shown below:

$$(P + S) >> k_d/k_f$$

$$k_{obs} = k_d E_t/(P + S)$$

$$k_d = k_{obs}(P + S)/E_t$$

At high ionic strength however, there is essentially no Cc:CcO complex present at equilibrium and the equation can be simplified as shown below:

$$(P + S) << k_d/k_f$$

$$k_{obs} = k_f E_t$$

$$k_f = k_{obs}/E_t$$

Steady state reactions were observed in low ionic strength and high ionic strength conditions. Low ionic strength conditions consisted of a 2 mM P_i buffer at pH=7, while high ionic strength

conditions costed of a 20 mM P_i buffer with 200 mM NaCl. In each trial, 300 µl of buffer was placed in a cuvette, and then the spectrophotometer was blanked. A different Cc species was then added, and the concentration was determined.

Low Ionic Strength Conditions

After experiments were run, data was analyzed to solve for rates and dissociation constants at low ionic strength conditions. The results of these experiments can be seen in **Table 4.**

Sample	Sample Type	[Cc] uM	Vol Oxidase (µl)	**Rate (s^{-1})**	[CcO] uM	**k_d (s^{-1})**
C	WT Horse	0.9	2	**0.0250**	0.0073	**3.08**
D	WT Horse	0.59	2	**0.0554**	0.0073	**4.48**
H	WT Horse	0.78	2	**0.0389**	0.0073	**4.16**
K	WT Horse	0.8	2	**0.0286**	0.0073	**3.13**
A	WT Human	0.87	1	**0.0102**	0.0037	**2.40**
B	WT Human	0.61	2	**0.0351**	0.0073	**2.93**
G	WT Human	0.46	2	**0.0173**	0.0073	**1.09**
J	WT Human	0.61	2	**0.0195**	0.0073	**1.63**
E	Y46E Human	0.57	2	**0.0191**	0.0073	**1.49**
F	Y46E Human	0.71	2	**0.0162**	0.0073	**1.58**
L	Y46E Human	0.53	2	**0.0154**	0.0073	**1.12**

Table 4. Comparison of reaction rates and dissociation rate constants between WT Horse Cc, WT Human Cc, and Y46E Cc at low ionic strength conditions.

For each Cc species, a graph of concentration over time after the addition of CcO to the sample was plotted. These can be seen in **Figures 8,9,10**.

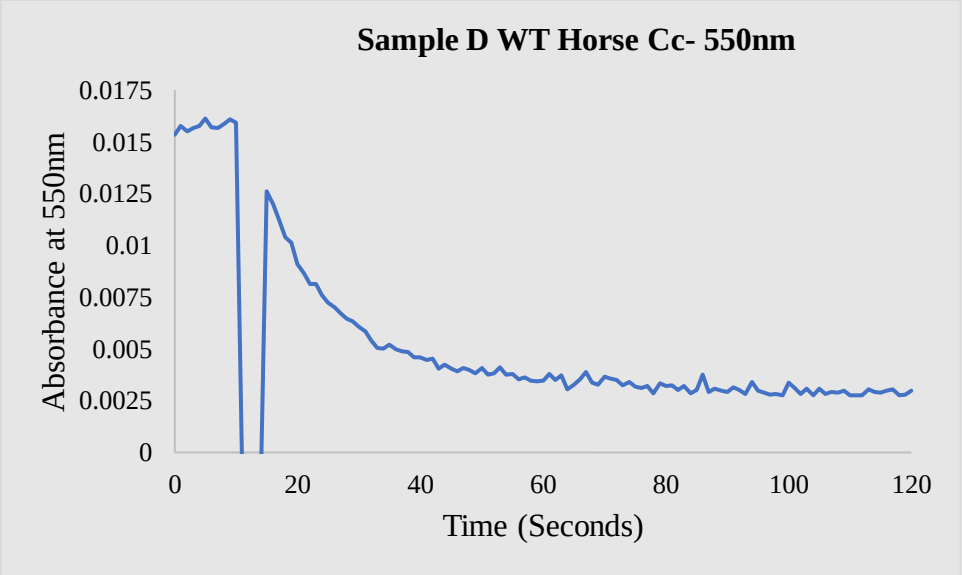

Figure 8. Concentration of WT Horse Cc (0.59 μM) as a function of time after addition of Bovine CcO (0.0073 μM) at low ionic strength. The observed rate is 0.0554 s^{-1}.

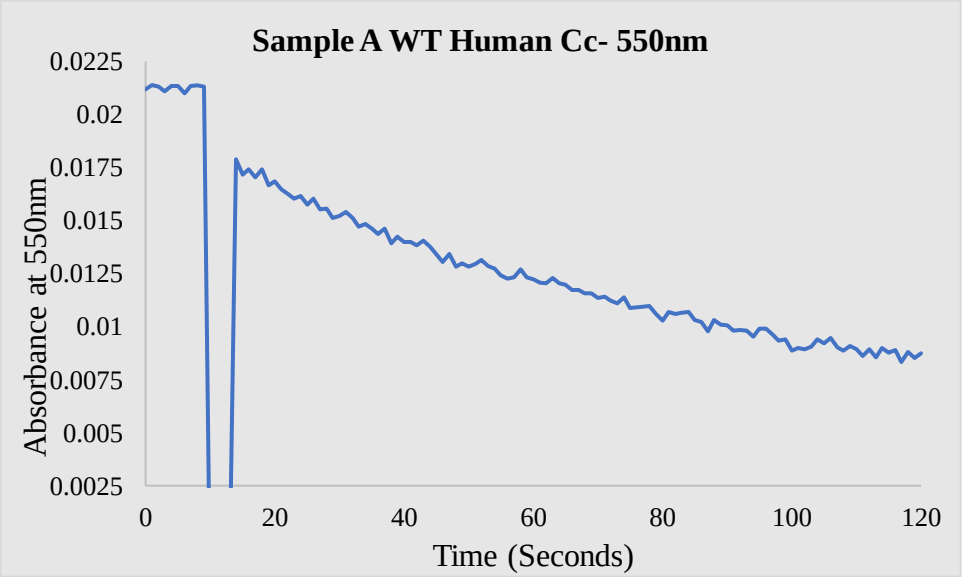

Figure 9. Concentration of WT Human Cc (0.87 μM) as a function of time after addition of Bovine CcO (0.0037 μM) at low ionic strength. The observed rate is 0.0102 s^{-1}.

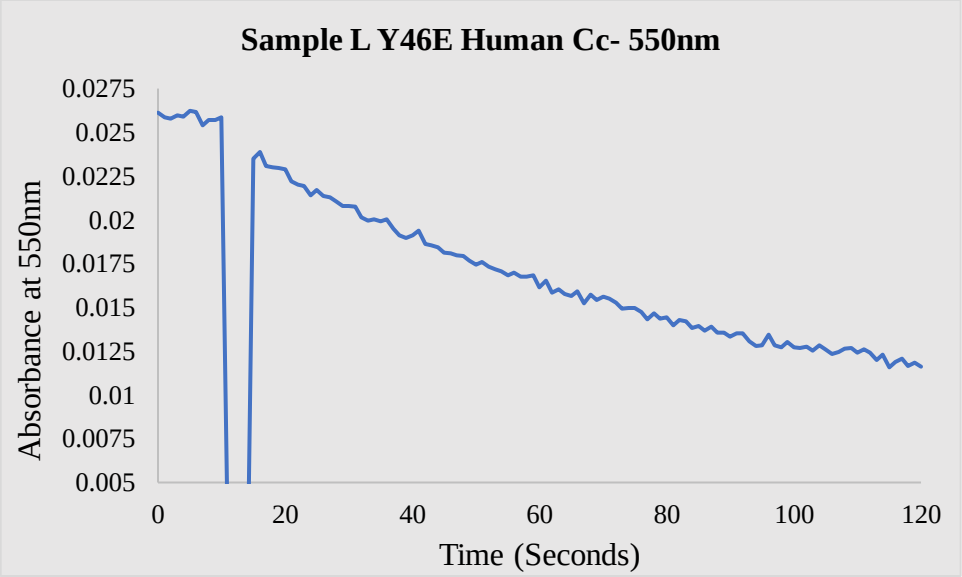

Figure 10. Concentration of Y46E Human Cc (0.53 μM) as a function of time after addition of Bovine CcO (0.0073 μM) at low ionic strength. The observed rate is 0.0154 s^{-1}.

High Ionic Strength Conditions

Steady state experiments were then repeated using high ionic strength conditions. These data can be found in **Table 5.**

Sample	Sample Type	[Cc] uM	Vol CcO (µl)	**Rate (s^{-1})**	[CcO] (uM)	**k_f ($mM^{-1}s^{-1}$)**
A	WT Horse	0.82	2	**0.0377**	0.0073	**5.16**
D	WT Horse	0.48	2	**0.0351**	0.0073	**4.81**
G	WT Horse	0.61	2	**0.0386**	0.0073	**5.29**
B	WT Human	0.52	2	**0.0649**	0.0073	**8.89**
E	WT Human	0.21	2	**0.0678**	0.0073	**9.29**
H	WT Human	0.45	2	**0.0520**	0.0073	**7.12**
C	Y46E Human	1.12	2	**0.0453**	0.0073	**6.21**
F	Y46E Human	0.36	2	**0.0604**	0.0073	**8.27**
I	Y46E Human	0.52	2	**0.0528**	0.0073	**7.23**

Table 5. Comparison of reaction rates and rates of formation between WT Horse Cc, WT Human Cc, and Y46E Cc at high ionic strength conditions.

Cc concentrations as a function of time after the addition of CcO were then plotted high ionic strength conditions. This can be seen in **Figures 11,12,13.**

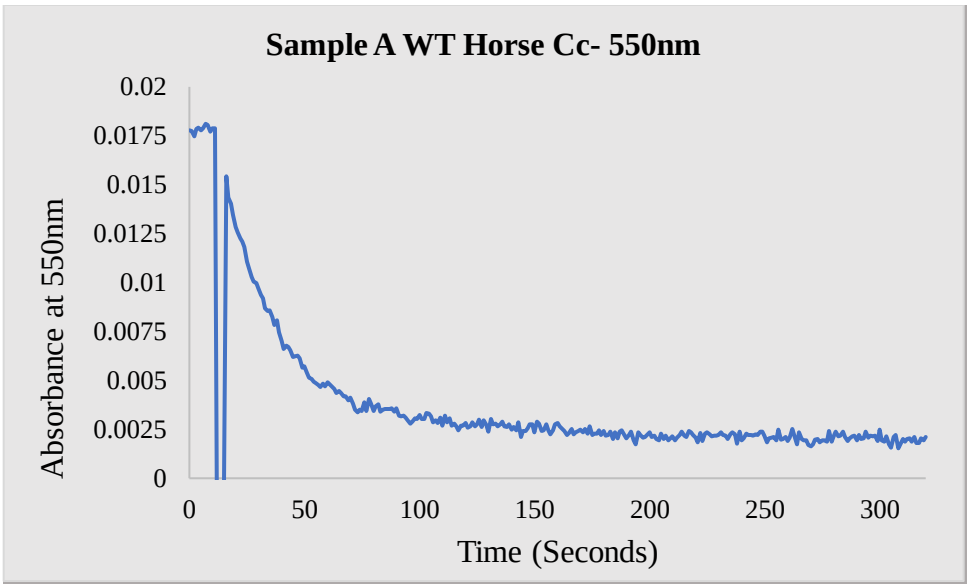

Figure 11. Concentration of WT Horse Cc (0.82 μM) as a function of time after the addition of CcO (0.0073 μM) at high ionic strength conditions. The observed rate is 0.0377 s^{-1}

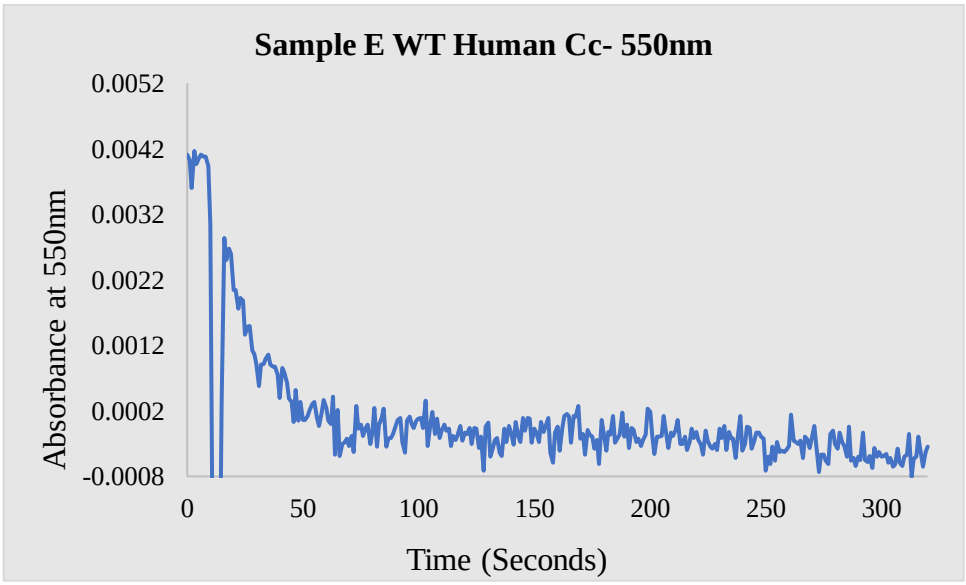

Figure 12. Concentration of WT Human Cc (0.21 μM) as a function of time after the addition of CcO (0.0073 μM) at high ionic strength conditions. The observed rate is 0.0678 s^{-1}.

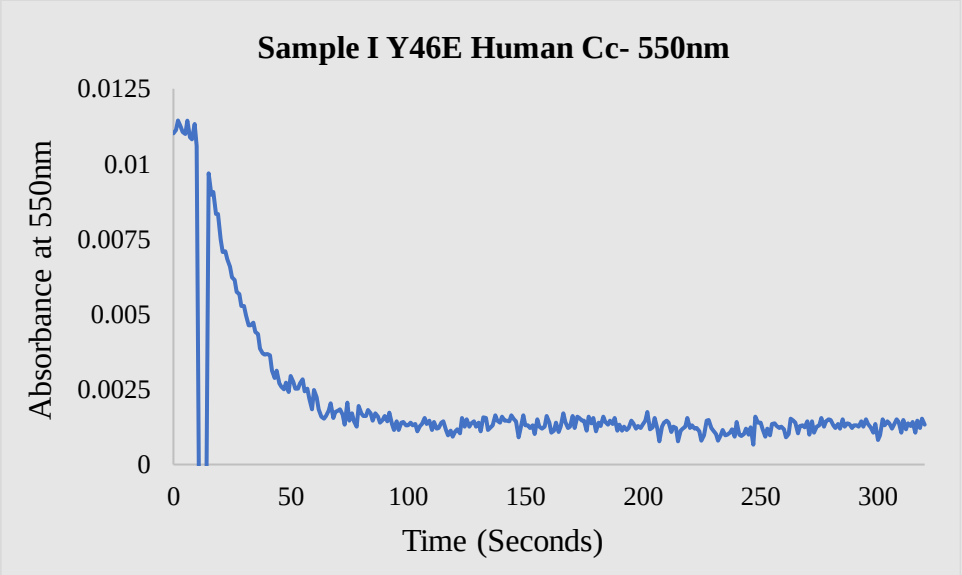

Figure 13. Concentration of Y46E Human Cc (0.52 μM) as a function of time after the addition of CcO (0.0073 μM) at high ionic strength conditions. The observed rate is 0.0528 s^{-1}.

This steady-state kinetics data has been summarized in **Table 6**, using the mean values and standard errors of each species at low ionic strength conditions and high ionic strength conditions.

Species	k_d (Low Ionic)	k_f (High Ionic)
WT Horse	3.71 +/- 0.36	5.09 +/- 0.14
WT Human	2.01 +/- 0.41	8.43 +/- 0.67
Y46E	1.40 +/-0.14	7.24 +/- 0.59

Table 6. Mean and standard errors for all species at low and high ionic strength conditions.

As the data shows in **Table 6**. WT Human Cc on average has a smaller k_d than WT Horse Cc. This indicates that the WT Human Cc binds more tightly than horse and has a slower rate at low ionic strength conditions. The k_d for Y46E Cc is slightly smaller on average than WT Human

Cc, but it is not large enough to determine specific differences in the binding kinetics between the two. At high ionic conditions however, k_f for WT Human Cc is almost two times larger on average than WT Horse Cc. This is consistent with previous studies and indicates the rate of formation is faster in WT Human Cc than in WT Horse Cc. Once again, the difference of Y46E Cc k_f at high ionic strength is too small to determine specific differences in binding kinetics.

Analytical Ultracentrifuge

During centrifugation, absorbance readings were taken at 410 nm every 10 minutes, for a total run time of about an hour per each salt condition. For each salt condition, a spike was recorded in the graph around 6.3 mm which indicates the approximate location of the centrifuge cell meniscus. Also, for each salt condition a plateau is observed around 6.55 mm. Analytical ultracentrifuge data is shown in **Figures 14 and 15.**

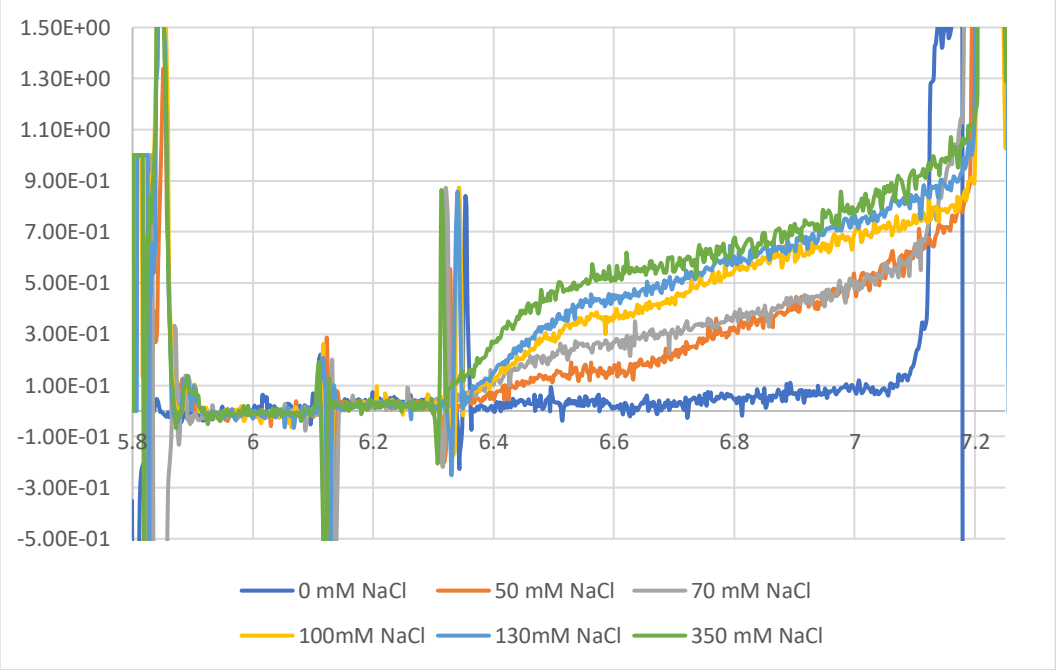

Figure 14. Analytical Ultracentrifuge data for WT Human Cc and Bovine CcO

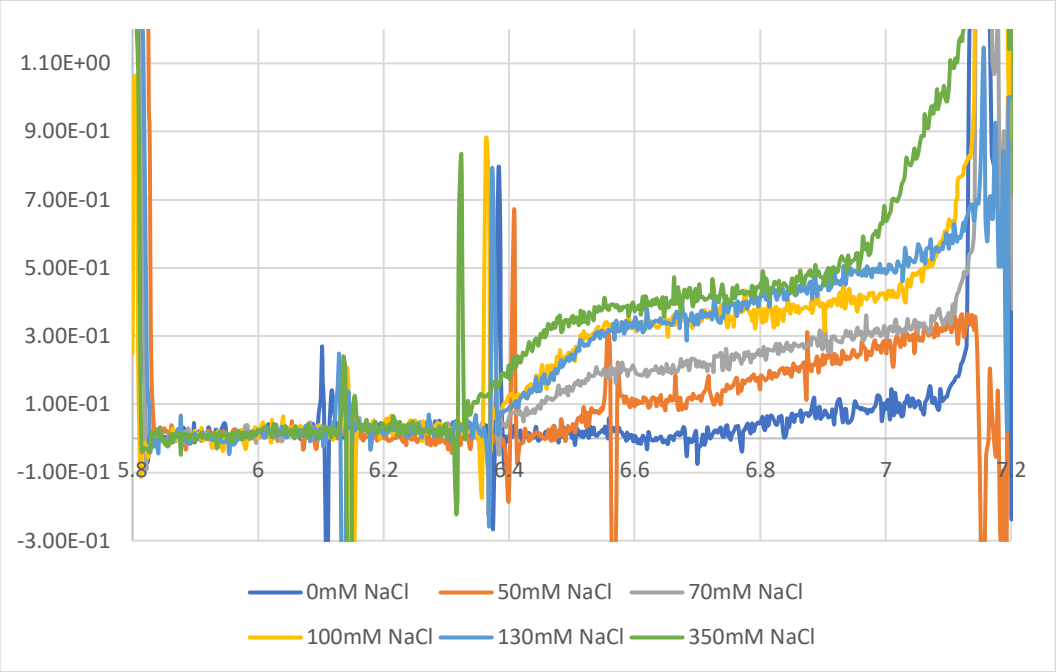

Figure 15. Analytical Ultracentrifuge data for Y46E Cc and Bovine CcO

Free [Cc] was calculated using the absorbance at the plateau (average), the [CcO] at baseline, and an extinction coefficient of 106.1 $mM^{-1}cm^{-1}$. This is shown in **Equation 4.**

$$\text{Free Cc} = \left[\frac{(\text{Plateau AU} - \text{Baseline [Cox]}}{106.1}\right] \times 1000$$

Free [CcO] was found by using **Equation 5.**

$$\text{Free [CcO]} = \text{Dilution [CcO]} - \text{Dilution [Cc]} - \text{Free [Cc]}$$

K_D values for each salt concentration were then able to be determined using **Equation 6.**

$$K_D = \frac{\text{Free [Cc]} \times \text{Free[CcO]}}{\text{Bound [Cc][CcO]}}$$

These values for both WT Human Cc and Y46E Human Cc are shown in **Table 7.**

[NaCl] mM	WT Human Cc K_D (μM)	Y46E Mutant K_D (μM)
0	0	0
50	1.40	2.26
70	4.15	4.84
100	11.53	30.45
130	28.82	32.55
350	NA	NA

Table 7. K_D Values for Y46E Cc and WT Cc at varying [NaCl]

K_D values are significant because they explain levels of bound and unbound proteins. Larger K_D values indicate higher concentrations of free protein and lower concentrations of bound protein. The Cc species with the higher K_D value would indicate a weaker binding complex with CcO. While Y46E K_D values at 50 mM NaCl and 70 mM NaCl are slightly larger than WT Human Cc K_D values, there is not a significant enough difference to suggest any significant binding differences. The K_D values at 100, 130, and 350 mM NaCl are insignificant because at that NaCl concentration it is assumed that Cc is completely unbound to CcO.

Conclusions

This research aimed to study the effects of the Cc phosphomimetic mutation Y46E and its binding with CcO. At low ionic strength conditions, steady state kinetic studies showed that WT Human Cc has a smaller k_d on average than WT Horse Cc, while Y46E Cc did not differ significantly from WT Human Cc. At high ionic conditions, k_f for WT Human Cc is almost twofold larger on average than WT Horse Cc, indicating that the rate of formation is faster in WT Human Cc. Y46E k_f values were not significantly different from WT Human Cc, indicating that our mutation did not have observable binding effects.

K_D values in ultracentrifuge experiments show the levels of bound and unbound proteins. At 50 mM NaCl and 70 mM NaCl, Y46E had a small increase in K_D. However, this difference cannot be attributed to actual binding properties since it is relatively small. There is a possibility that Y46E binds weaker than WT Human Cc, but this research did not give clear results. The values at 100,130, and 350 mM NaCl are not included in data analysis because it is assumed that Cc is completely unbound from CcO.

Studying the binding effects of mutated Cc residues could have key implications for future research into treatment of post-ischemic reperfusion injuries. While our specific phosphomimetic mutant did not show significant effects, it is possible that further study into this mutant or others could reveal larger binding differences that could be useful in targeted disease treatments. The study of Cc and its various functions are currently under many areas of research. Recently, Chen et al have extensively studied ROS overproduction and how all the various parts of the ETC are interconnected, with hopeful progress in therapeutic target treatments for cardiovascular disease (Chen, Zhang, Jin, Kasumov, & Chen, 2022). More research will be needed in the areas of the

ETC, ROS overproduction, and the specific physiological consequences of ischemia-reperfusion injuries, but advances in this research could cause dramatic changes in the treatment of disease.

Bibliography

García-Heredia, J., Díaz-Quintana, A., Salzano, M., Orzáez, M., Pérez-Payá, E., Teixeira, M., . . . Díaz-Moreno, I. (2011). Tyrosine phosphorylation turns alkaline transition into a biologically relevant process and makes human cytochrome c behave as an anti-apoptotic switch. *Journal of biological inorganic chemistry*, 1155-1168.

Guerra-Castellano, A., Díaz-Quintana, A., Pérez-Mejías, G., Elena-Real, C. A., González-Arzola, K., García-Mauriño, S. M., . . . Díaz-Moreno, I. (2018). Oxidative stress is tightly regulated by cytochrome c phosphorylation and respirasome factors in mitochondria. *Biophysics and Computational Biology*, 7955-7960.

Hüttemann, M., Helling, S., Sanderson, T. H., Sinkler, C., Samavati, L., Mahapatra, G., . . . Lee, I. (2012). Regulation of mitochondrial respiration and apoptosis through cell signaling: Cytochrome c oxidase and cytochrome c in ischemia/reperfusion injury and inflammation. *Biochimica et Biophysica Acta (BBA)- Bioenergetics, 1817*(4), 598-609.

Hüttemann, M., Pecina, P., Rainbolt, M., Sanderson, T., Kagan, V. E., Samavati, L., . . . Lee, I. (2011). The multiple functions of cytochrome c and their regulation in life and death decisions of the mammalilan cell: From respiration to apoptosis. *Mitochondrion, 11*(3), 369-381.

Kaim, G., & Dimroth, P. (1999). ATP synthesis by F-type ATP synthase is obligatorily dependent on the transmembrane voltage. *European Molecular Biology Organization*, 4118-4127.

Kalpage, H. A., Bazylianska, V., Recanati, A. M., Fite, A., Liu, J., Wan, J., . . . L. (2019). Tissue-specific regulation of cytochrome c by post-translational modifications: respiration, the mitochondrial membrane potential, ROS, and apoptosis. *Federation of American Societies for Experimental Biology*, *33*(2), 1540-1553.

Kalpage, H. A., Vaishnav, A., Liu, J., Varughese, A., Wan, J., Turner, A. A., . . . Sanderson, T. (2019). Serine-47 phosphorylation of cytochrome c in the mammalian brain regulates cytochrome c oxidase and caspase-3 activity. *Federation of American Societies for Experimental Biology*.

Kalpage, H. A., Wan, J., Morse, P. T., Zurek, M. P., Turner, A. A., Khobeir, A., . . . Edwards, B. F. (2020). Cytochrome c phosphorylation: Control of mitochondrial electron transport chain flux and apoptosis. *International Journal of Biochemistry and Cell Biology, 121*, 105704.

Lee, I., Salomon, A. R., Doan, J. W., Grossman, L. I., & Hütteman, M. (2006). New Prospects for an Old Enzyme: Mammalian Cytochrome c Is Tyrosine-Phosphorylated in Vivo. *Biochemistry, 45*(30), 9121-9128.

Mahapatra, G., Varughese, A., Ji, Q., Lee, I., Liu, J., Vaishnav, A., . . . Brunzelle, J. (2017). Phosphorylation of Cytochrome c Threonine 28 Regulates Electron Transport Chain Activity in Kidney: IMPLICATIONS FOR AMP KINASE. *Journal of Biological Chemistry*, 64-79.

Minnaert, K. (1961). The kinetics of cytochrome c oxidase I. The System: Cytochrome C-Cytochrome Oxidaseoxygen. *Biochimica et Biphysica* , 23-34.

Pecina, P., Borisenko, G. G., Belikova, N. A., Tyurina, Y. Y., Pecinova, A., Lee, I., . . . Hüttemann, M. (2010). Phosphomimetic substitution of cytochrome C tyrosine 48 decreases respiration and binding to cardiolipin and abolishes ability to trigger downstream caspase activation. *Biochemistry*, 6705-6714.

Roberts, V. A., & Pique, M. E. (1999). Definition of the interaction domain for cytochrome c on cytochrome c oxidase. III. Prediction of the docked complex by a complete, systematic search. *Journal of Biological Chemistry, 274*(53), 38051-38060.

Scharlau, M., Geren, L., Zhen, E. Y., Ma, L., Rajagukguk, R., Miller, S. F., . . . Millett, F. (2019). Definition of the Interaction Domain and Electron Transfer Routebetween Cytochrome c and Cytochrome Oxidase. *Biochemistry, 58*(40), 4125-4135.

Shimada, S., Itoh, K. S., Baba, J., Aoe, S., Shimada, A., Yamashita, E., . . . Tsukihara, T. (2017). Complex structure of cytochrome c–cytochrome c oxidase reveals a novel protein–protein interaction mode. *EMBO*, 291-300.

Smith, H. T., Ahmed, A., & Millett, F. (1981). Electrostatic interaction of cytochrome c with cytochrome c1 and cytochrome oxidase. *Journal of Biological Chemistry*, 4984-4990.

Smith, L., Davis, H. C., & Nava, M. E. (1979). Studies of the kinetics of oxidation of cytochrome c by cytochrome c oxidase: Comparison of spectrophotometric and polarographic assays. *American Chemical Society*, 3140-3146.

Wan, J., Kalpage, H. A., Vaishnav, A., Liu, J., Lee, I., Mahapatra, G., . . . Hüttemann. (2019). Regulation of Respiration and Apoptosis by Cytochrome c Threonine 58 Phosphorylation. *Scientific Reports*, 15815.

Yu, H., Salomon, A. R., Yu, K., & Hüttemann, M. (2008). Mammalian liver cytochrome c is tyrosine-48 phosphorylated in vivo, inhibiting mitochondrial respiration. *Biochemica et Biophysica Acta (BBA)- Bioenergetics* , 1066-1071.

Zhao, R. Z., Jiang, S., Zhang, L., & Yu, Z. B. (2019). Mitochondrial electron transport chain, ROS generation and uncoupling (Review). *International Journal of Molecular Medicine*, 3-15.